Catalysis Science & Technology

Accepted Manuscript

ROYAL SOCIETY OF CHEMISTRY

www.rsc.org/catalysis

Catalysis Science and Technology

ARTICLE

Catalysts based on TiO_2 anchored with MoO_3 or SO_4^{2-} to Conversion of Cellulose into Chemicals

Received 00th January 20xx,
Accepted 00th January 20xx

DOI: 10.1039/x0xx00000x

www.rsc.org/

R. M. de Almeida[a], N. J. A. de Albuquerque[a], F. T. C. Souza[a] and S. M. P. Meneghetti[a]

Biomass is comprised of a high percentage of cellulosic material, with great potential for transformation into chemical reagents, and thus it is of interest to the chemical, food, medical and fuel industries. The conversion of cellulose was evaluated in the presence of solid acid catalysts based on TiO_2 anchored with MoO_3 and SO_4^{2-}. The catalysts were characterized by infrared and Raman absorption spectroscopy, pyridine-adsorption infrared spectroscopy, thermogravimetric analysis and by the N_2 adsorption–desorption isotherms and the determination of the temperature-programmed desorption of NH_3 (NH_3-TPD). The catalysts showed low to moderate acid sites: TiO_2/MoO_3-30 > TiO_2/SO_4^{2-}-35 > TiO_2/SO_4^{2-}-25 > TiO_2, and the cellulose conversion was between 27 and 35 %.

Introduction

Biomass is an important source of energy and chemicals, but the traditional uses of this resource, involving non-sustainable consumption and low efficiency conversion, require further research and development. Thus, the modern use of biomass will be dependent on new conversion processes becoming technically and economically viable, or even increasing the scale and overcoming the technological barriers associated with the traditional processes[1-3]. Biomass has great potential for transformation into chemicals, since it is comprised of a high percentage of cellulosic material and thus it is of interest to the chemical, food, medical and fuel industries[4-9]. A notable potential application is the conversion of cellulose through hydrolysis to obtain glucose and coproducts such as fructose, 5-hydroxymethylfurfural, organic acids and 1,6-anhydroglucose. These coproducts are obtained based on parallel reactions of the transformation of glucose by isomerization, dehydration, hydration, among others[10,11]. In studies carried out recently, the hydrolysis of cellulose to obtain glucose and coproducts has been carried out using enzymatic, dilute acid and basic catalysts, in some cases under supercritical conditions[6,12-14]. Relatively few studies have involved heterogeneous acid catalysts, such as Pt/Na (H)-ZSM-5 and Pt/Carbon[10], Pt/c-Al_2O_3[16], Ru/C[17], Ru/CNT[18,19], Ru/C and Ru/USY[20-23]. In other studies Onda et al., Huang et al. and Shen et al. carried out cellulose hydrolysis reactions using solid acid catalysts, such as zeolite, W/SiO_2-Al_2O_3, sulfonated catalysts, and others[24-28]. Studies on the conversion of biomass using TiO_2 include the modification of their surface aiming to change the physical-chemistry properties, leading to species exhibiting catalytic activity. TiO_2-ZrO_2 catalysts mainly yielding hydroximethylfurfural, furfural, anhydroglucose, glucose and fructose, however, under hydrothermal conditions at 473 to 673 K[29]. As in the case of the magnetic catalyst SO_4^{2-}/TiO_2-Fe_3O_4, in the conversion of cellulose, TiO_2 in carbon nanotubes and enzymes provide sugars in around 80 % yield [30,31]. Watanabe et al. specify some possible routes using TiO_2 in the dehydration of glucose as the main product of cellulose hydrolysis, at a temperature of 473 K[32]. Kobayashi et al. used Pt/TiO_2 in cellulose conversion reactions at a temperature of 190 °C, $P(H_2)$ = 5.0 Mpa and a reaction time of 24 h, with yields of fermentable sugars of 26.2 % and 78.8 % in cellulose conversion[33].

Thus, in this context, this work intend to investigate the effect of the presence of MoO_3 and SO_4^{2-} on TiO_2 matrix, in order to increase the acidity of the TiO_2. These materials were employed as acid catalysts in the conversion of cellulose into products of industrial interest, mainly sugars.

Results and discussion

Characterization of catalysts

Based on the thermogravimetric analysis (Figure 1), the percentages (by mass) of MoO_3 and SO_4^{2-} present in the catalysts were determined. The sulfated catalysts (Fig. 1(a)) showed mass losses of 25 and 35 % related to sulfate in the temperature range of 470 to 650 °C[43] and the catalyst containing molybdenum (Fig. 1(a)) showed a mass loss of 30 % related to molybdenum oxide in the temperature range of 780 to 850 °C[44]. Two mass loss events can be observed on the first derivative curves obtained for the catalysts in the temperature ranges related to sulfate and molybdenum oxide loss, respectively. These events are associated with the presence of monodentate or bidentate sulfates (bridge or chelate) coordinated to TiO_2[34,35] and for the catalyst with molybdenum

[a] *Grupo de Catálise e Reatividade Química, Instituto de Química e Biotecnologia, Universidade Federal de Alagoas, Campus A.C. Simões, Av. Lourival de Melo Mota, Maceió/AL. CEP: 57072-970. E-mail: rusiene.almeida@iqb.ufal.br: Fax: +55 82 3214 1384; Tel: +55 82 3214 1703.*

† Electronic Supplementary Information (ESI) available: Experimental details and supporting data of TGA, FTIR, TPD-NH_3, FTIR with pyridine adsorption, Raman Spectroscopy and High-performance liquid chromatography. See DOI: 10.1039/x0xx00000x

oxide this may be associated with the presence of different molybdenum oxides[36].

Insert **Figure 1**

The infrared absorption spectrum for the catalyst TiO_2/MoO_3-30 (Fig. 2) shows bands related to the crystalline bulk of MoO_3[39,40]: 991, 897 and 819 cm^{-1} and the catalysts containing sulfate show bands associated with the sulfates coordinated in the bidentate form, both bridge and chelate[34,35]. Thus, the events observed on the first derivative mass loss curves for the catalysts are associated with these structures[34,35].

Insert **Figure 2**

On the Raman spectra for the catalysts (Fig. 3) signals can be observed at 146, 398, 514 and 637 cm^{-1} which are characteristic of TiO_2 in the crystalline anatase[41]. For the catalyst TiO_2/MoO_3-30, besides the anatase indication, other signals at 188, 287, 338, 379, 666, 824 and 999 cm^{-1} are present, associated with the vibration modes $A_g - \delta (O_2Mo_2)_n$, $B_{3g} - \delta$ (OMo), $A_g - \delta (OMo_3)$, B_{1g} - $\upsilon(OMo_3)$, B_{3g} - $\upsilon(OMo_3)$, B_{1g} - $\upsilon(OMo_2)$, $A_{1g} - B_{1g}$, υ(OMo), respectively. The presence of these signals indicates the formation of tetrahedral molybdates corresponding to the orthorhombic phase of MoO_3[35] .

Insert **Figure 3**

On the absorption spectra obtained for the catalyst, at the medium infrared region, bands are present at 1486, 1536 and 1606 cm^{-1} characteristic of coordinated and adsorbed pyridine[46]. However, the sulfate catalysts showed weak intensity for these bands (Fig. 4), suggesting less strength for these acid sites when compared with the catalyst containing Mo. The TiO_2/MoO_3-30 catalyst showed greater acid strength, since the band intensities related to the pyridine adsorbed onto the Lewis and Brönsted acid sites remained intense at 190 °C.

The ratio between the band intensities related to the Lewis (1606 cm^{-1}) and Brönsted acid sites (1536 cm^{-1}), I_L/I_B, allows the density of the predominant acid sites of the catalyst to be estimated[46]. In Table 1, the I_L/I_B rations are listed. The TiO_2/MoO_3-30 catalyst exhibiting the superior Brönsted acidity follows the TiO_2/SO_4^{2-}-25 and TiO_2/SO_4^{2}-35, since I_L/I_B = 0.62, 0.95 and 1.02, respectively. For the sulfated catalysts the increased sulfated concentration didn't affect the predominance of Lewis acidity. To complete discussion about strength acidity was used the TPD-NH_3, following.

The curves for the temperature-programmed desorption of NH_3 (NH_3-TPD) show the influence of the anchorage of the sulfate and molybdenum oxide to the TiO_2 (Fig. 5(a)), since the TiO_2 showed lower intensity on the ammonia desorption curve. The ammonia desorption temperature for the catalysts containing sulfate was in the range of 100 to 450 °C, attributed to the weak and moderate acid sites[47-49]. It should be noted that above 450 °C, the sulfated catalysts suffer thermal degradation (Fig. 1) and was not possible to obtain NH_3-TPD curve until 900 °C. Though, the possibility that moderate to strong sites are present cannot be rejected. The catalyst containing molybdenum, besides weak and moderate acid sites also showed the presence of strong acid sites, with a NH_3-TPD temperature of up to 700 °C [47-49].

Insert **Figure 4**

Insert **Table 1**

Figure 5b shows the strength of the acid sides, considering the peak area obtained from the NH_3-TPD as a function of the catalyst mass, used in the cellulose conversion reactions ($2.69.10^{-5}$ mol of catalyst). The order of the values obtained for the total acidity of the reaction media, considering just the quantity of weak to moderate acid sites was: TiO_2/MoO_3-30 > TiO_2/SO_4^{2-}35 > TiO_2/SO_4^{2-}-25 > TiO_2. The anchorage of MoO_3 favored an increase in the density of the sites with moderate to strong acid characteristics. This characteristic is related to the confinement of the hydroxyls present on the TiO_2 surface, forming a monodentate species which carry a proton (hydrogen atom) in its structure, which acts as a Brönsted acid center[61]. These results are consistent with the infrared absorption spectra with pyridine adsorbed onto the catalysts, since only the catalyst with MoO_3 showed at a band at 1605 cm^{-1} and a greater intensity for the band at 1536 cm^{-1}, attributed to the Brönsted acid sites. For the catalysts containing SO_4^{2-} there was an increase in the acid strength due to the inductive effect of the sulfate on the metal cation, which becomes more deficient in electrons contributing to the increase in the strength of the Lewis acid sites[62].

Insert **Figure 5**

Evaluation of catalytic activity

In Fig. 6, a cellulose conversion of 15 % can be observed without the use of a catalyst, due to the action of the water molecules as a catalyst, under the reaction conditions employed[51]. With the use of sulfuric acid, a cellulose conversion of 25 % was observed, due to the high acidity and solubility in water. The use of TiO_2 led to a conversion of 20 %, which could be associated with the acidity of the material (NH_3-TPD, Fig 5(a)).

The modified catalysts showed higher activity compared with those observed for H_2SO_4 and TiO_2 or in the absence of a catalyst. In the case of TiO_2/MoO_3-30 and TiO_2/SO_4^{2-}-35 a cellulose conversion of 35 % was obtained and for the catalyst TiO_2/SO_4^{2}-25 the conversion was 27 %. These data suggest that the catalytic activity is associated with the presence of Lewis

and Brönsted sites, exhibiting weak to moderate characteristics (Fig. 5). However, the influence of strong acid sites cannot be discarded. Although TiO_2/MoO_3-30 shows higher acidity (Fig. 5) and stronger Brönsted acid sites (Table1) compared with the sulfated catalysts, the results for the cellulose conversion were similar to those obtained for TiO_2/SO_4^{2-}-35. Similarly, Chambon et al. showed that the catalysts containing Lewis and Brönsted acid sites promoted an increase in the cellulose conversion compared with those containing only Brönsted acid sites. This tendency may be related to the depolymerization as well as the hydrolysis reactions, solubilization and cellulose degradation, promoted by the synergism between the Lewis and Brönsted acid sites, forming soluble oligomers and polymers, short-chain carbohydrates, organic acids and furanic compounds, among others[60].

Insert **Figure 6**

In Figure 7, data on the percentage yield of the major products which are soluble in water obtained in the cellulose conversion reaction are also shown. In the absence of a catalyst the formation of mainly glucose and small quantities of fructose, cellobiose, 5-HMF, 1,6-anhydroglucose and organic acids (formic and acetic) was observed. In the presence of H_2SO_4, there is a notable formation of glucose and 5-HMF, along with small quantities of fructose, cellobiose, 1,6-anhydroglucose and formic and acetic acids.

In the presence of TiO_2 the major products formed were similar to those observed with the use of H_2SO_4 or in the absence of a catalyst. However, for the modified catalysts, TiO_2/SO_4^{2-}-35 showed the highest glucose yield, followed by TiO_2/SO_4^{2-}-25 and TiO_2/MoO_3-30. It should be noted that in the presence of the modified systems the formation of lactic acid and 1,6-anhydroglucose was observed, products which were not detected in the absence of a catalyst or with the use of TiO_2 and H_2SO_4. Considering the data on the acidity of the media in NH_3-TPD the following order was observed: TiO_2/MoO_3 - 30 > TiO_2/SO_4^{2-} - 35 > TiO_2/SO_4^{2-} - 25 > TiO_2 and thus it appears that the low glucose yield obtained with the catalyst TiO_2/MoO_3-30 is associated with the total acidity of the catalyst, which is higher than that of the other catalysts used. This characteristic leads to the transformation of glucose into other products through dehydration, hydration, isomerization and epimerization reactions, among others, which explains the higher content of lactic acid and 1,6-anhydroglucose observed with the use of TiO_2/MoO_3-30.

Experimental

Synthesis of TiO_2/MoO_3 and TiO_2/SO_4^{2-} catalysts

TiO_2 was obtained via the sol-gel process followed by the anchoring of MoO_3 and SO_4^{-2} [36,37]. Two solutions were prepared: 1) 37.7 ml of isopropanol (Vetec) and 2.3 ml of deionized water; and 2) 37.7 ml of isopropanol (Vetec), 18.7 ml of titanium isopropoxide (Sigma Aldrich) and 3.33 ml of 70 % HNO_3 (Vetec). Solution 1 was added slowly to solution 2 under stirring and after a few seconds a gel was formed, which was left to age for 2 h, followed by drying at 90 °C for 4 h and calcination at 550 °C for 4 h in air. For the impregnation of MoO_3 and SO_4^{2-} over TiO_2, solutions were prepared with 0.65 g of ammonium molybdate (Sigma Aldrich) in 20 mL of deionized water and 0.35 mL – 0.80 mL of sulfuric acid (Vetec) in 12 mL of water with 1 g of TiO_2. The solutions were kept under stirring for 1 h at 25 °C, followed by heating at 90 °C, for the evaporation of water, and calcination at 550 °C for 4 h in air. The catalysts synthesized are referred to herein as TiO_2/MoO_3-X and TiO_2/SO_4^{2-} - X, where X corresponds to 30 % of MoO_3 and 25 and 35 % of SO_4^{2-} (determined experimentally).

Insert **Figure 7**

Characterization of catalysts

The absorption spectra in the infrared region of the catalysts with pyridine adsorbed were obtained using a Varian infrared spectrophotometer (model IR 660) equipped with an ATR accessory. The thermogravimetric analysis was carried out on a Shimadzu analyzer (model TGA-50) under an N_2 atmosphere with a heating rate of 10 °C.min^{-1}. The Raman spectra were obtained on a Renishaw System (inVia Raman) with an RL 633 Renishaw Class 3B HeNe laser. The temperature programmed desorption of NH_3 (TPD-NH_3) analysis was carried out on a Quantachrome Instruments analyzer (model ChemBET 3000) with thermal conductivity.

Cellulose conversion and calculation of yield of soluble products obtained

The tests on the catalytic conversion of cellulose were conducted at 190 °C/4 h in a 100 mL stainless steel reactor, coupled to a monometer, temperature probe and magnetic stirrer (1000 rpm). The following amounts were used: 0.48 g of cellulose in 60 mL of deionized water and 2.69 x 10^{-5} mol of catalyst[11]. After the catalytic tests, the residual solid was filtered and dried at 90 °C for 24 h. The cellulose conversion and the detection of products were carried out according to the description of Dhepe and Fukuoka[16]. Based on an analysis of the reaction products by HPLC, the selectivity calculations were expressed using the equation: product yield (%) = (C_p/C_o) x C; where: C_p = concentration of product in the liquid phase (g/L), C = cellulose conversion (%) and C_o = initial cellulose concentration (g/L).

Conclusions

The anchorage of MoO_3 or SO_4^{2-} on TiO_2 led to an increase in the acidity and consequently an increase in the catalytic activity in the conversion of cellulose, with the notable presence of Lewis and Brönsted acid sites with weak to moderate acid characteristics. The most acidic modified catalysts led to the formation of lactic acid and 1,6-

anhydroglucose, products which were not observed with the use of TiO_2, H_2SO_4 or when no catalyst was employed.

Acknowledgements

Thank the National Counsel of Technological and Scientific Development (CNPq) for financial support.

Notes and references

1 X. X. Tong, X. P. Luo, L. M. Wu, C. X. Lin, W. H. Yu, C. H. Zhou, Z. K. Zhong and D. Shen, *Applied Clay Science*, 2013, **74**, 147-153.

2 D. Saikat and P. Sharmistha, *Biomass and Bioenergy*, 2014, **62**, 182-197.

3 F. Rosillo-Calle, S. V. Bajay and E. Rothman, *Editor of the University of Campinas- UNICAMP***,** 2005.

4 P. Yang, H. Kobayshi, A. Fukuoka, *Chinese Journal of Catalysis*, 2011, **32**, 716-722.

5 G. W. Huber, S. Iborra, A. Corma, *Chem. Rev*., 2005, **109**, 4044–4098.

6 D. Klemm, H. Hublein, H. Fink and A. Bohn, *Angew. Chem*., 2005, **44**, 3358–3393.

7 Y. P. Zhang and L. R. Lynd, *Biotechnology and bioengineering,* 2004, **88**, 797-824.

8 A. J. Ragauskas, C. K. Williams, B. H. Davison, G. Britovsek, J. Cairney, C. A. Eckert, W. J. Frederick, J. P. Hallett,D. J. Leak, C. L. Liotta, J.R. Mielenz, R. Murphy, R. Templer, T. Tschaplinski, *Science* , 2006, **311**, 484-489.

9 Davda, R.R.; Shabaker, J.W.; Huber, G.W.; Cortright, R.D.; AND DUMESIC, J.A., *Appl. Catal.,* B, 56, 171–186, 2005.

10 P. Yang, H. Kobayashi and A. Fukuoka*, Chinese Journal of Catalysis*, 2011, **32**, 716-722.

11 J. B. dos Santos, F. L. Silva, F. M. R. S. Altino, T.S. Moreira, M.R. Meneghetti and S.M.P. Meneghetti, *Catal*. *Sci. Technol.*, 2013, **3**, 673-678.

12 F. Chambon, F. Rataboul, C. Pinel, A. Cabiac, E. Guillon, N. Essayen, *Applied catalysis B: environmental*, 2011, **105**, 171-181.

13 S. Saka and T. Ueno, *Cellulose*, 1999, **6**, 177–191.

14 T. Sasaki, T. Adschiri and Arai, *Aiche Journal*, 2004, **50**, 192–202.

15 M. Fitzpatrick, P. Champagne, M.F. Cunningham, R.A. Whitney, *Bioresour. Technol.,* 2010, **101**, 8915–8922.

16 A. Fukuoka and P.L. Dhepe, *Angew. Chem.,* 2006, **45**, 5161–5163.

17 C. Luo, C. Wang and H. Liu, *Angew. Chem.,* 2007, **46**, 7636–7639.2007.

18 W. Deng, X. Tan, W. Fang, Q. Zhang and Y. Wang, *Catal.Lett*., 2009, **133**, 167–174.

19 H. Wang, L. Zhu, S. Peng, F. Peng, J. Yu, G.Yang, *Renew. Energy*, 2011, **37**, 192–196.

20 Y. Zhu, Z.N. Kong, L.P. Stubbs, H. Lin, S. Shen, E.V. Anslyn, J.A. Maguire, *Chem.Sus.Chem*., 2010, **3**, 67–70.

21 R. Palkovits, K. Tajvidi, J. Procelewska, R. Rinaldi, A. Ruppert, *Green Chem*., 2010, **12**, 972–978.

22 J. Geboers, S. Van de Vyver, K. Carpentier, K. de Blochouse, P. Jacobs and B. Sels, *Catal. Commun.,* 2010, **46**, 3577–3579.

23 J. Geboers, S. Van de Vyver, K. Carpentier, P. Jacobs and B. Sels, *Catal. Commun., 2011,* **47**, 5590–5592.

24 A. Onda, T. Ochi and K. Yanagisawa, *Green Chemisry,* 2008, **10**, 1033-1037.

25 H.B. Huang and Y. Fu, *Green Chem*., 2013, **15**, 1095–1111.

26 I. Gubaek, S. J. You and E. D. Park, *Bioresource Technology, 2012,* **114**, 684–690.

27 S. Shen, C. Wang, B. Cai, H. Li, Y. Han, T. Wang and H. Qin, *Fuel*, 2013, **113**, 644–649.

28 M. Yabushita, H. Kobayashi, A. Fukuoka, *Applied Catalysis B: Environmental*, 2014, **145**, 1-9.

29 A. Hareonlimkun, V. Champreda, A. Shotipruk and N. Laosiripojana, *Bioresource Technology*, 2010, **101**, 4179–4186.

30 H. Abushammala and R. Hashaikeh, *Biomass and bioenergy,* 2011, **35**, 3970-3975.

31 Q. Lu, X. N. Ye, Z.B. Zhang, C.Q. Dong and Y. Zhang*, Bioresource Technology*, 2014, **171**, 10–15.

32 M. Watanabe , Y. Aizawa, L. Iida, T.M. Ainda, C. Levy, K. Sue, H. Inomata, *Carbohydr. Res*. 2005, **340**, 1925-1930.

33 H. Kobayashi, Y. Ito, T. Komanoya, Y. Hosaka, P. L. Dhepe, K. Kasai, K. Haraa and A. Fukuoka, *Green Chem.,* 2011, **13**, 326.

34 V. Swamy, A. Kuznetsov, L.S. Dubrovinsky, R.A. Caruso, D.G. Shchukin and B.C. Muddle, *Phys. Rev*., 2005, **71**, 1–11.

35 G. Busca, G. Ramis, J.M. Gallardo, V.S. Escribano and P. Piaggio, *J. Chem. Soc*. , 1994, **90**, 3181–3190.

36 D. A. Ward and E.I. Ko, *Journal Catalysis*, 1994, **150**, 18 – 33.

37 H. Armendariz, B. Coq, D. Tichit, R. Dutartre and F. Figueras, *Journal of Catalysis,* 1998, *173*, 345–354.

38 V. Choudhary, S.H. Mushrif, C. Ho and V. Nikolakis, *Journal of the American Chemical Society*, 2013, **135**, 3997-4006.

39 M. Daturi and G.L. Appel, *Journal of Catalysis*, 2002, **209**, 427 – 432.

40 T. Ono, Y. Kakagawa, H. Miyata, Y. Kubokawa, *The chemical Society of Japan,* 1984, **57**, 1205 -1210.

41 G. Busca, G. Ramis, J.M.G. Amores, V.S. Escribano and P. Piaggio, *J.Chem. Soc.,* 1994, **90**, 3181–3190.

42 N. E. Boboriko and D. I. Michko, *Inorganic Material*, 2013, **49**, 795 – 801.

43 H. Zhao, S. Bennici, J. Shen and A. Auroux, *Applied Catalysis A: General*, 2009, **356**, 121 – 128.

44 H.G. El-Shobaky, M. Mokhtar and A. S. Ahmed, *Thermochim. Acta.*, 1999, **327**, 39–46.

45 X. Wang, J. Yu, P. Liu , X. Wang, W. Su and X. FU, *Journal of Photochemistry and Photobiology A: Chemistry* , 2006, **179**, 339–347.

46 R. M. Almeida, M.R. Meneghetti, S.M.P. Meneghetti, L.K. Noda and N.S. Gonçalves, *Applied Catalysis A: General*, 2008, **347**, 100 – 105.

47 C. Gannouna, A. Turki, H. Kochkar, R. Delaiglec, P. Eloyc, A. Ghorbel and E.M. Gaigneaux, *Applied Catalysis B: Environmental*, 2014, **147**, 58–64.

48 Y. Leng, Y. Zhang, C. Huang, X. Liu and Y. Wu, *Bull. Korean Chem. Soc*. 2013, **34**, 1-4.

49 C. L. Ping, L. Y. Jun, L. Zhong and Z. J. Fu, *J. Cent. South Univ*., 2014, **21**, 1719−1724.

50 N. Lavoine, I. Desloges, A. Dufresne and J. Bras, *Carbohydrate polymers*, 2012, 90, 735-764.

51 Y. Yu, X. Lou and H. Wu, *Energy &Fuel*, 2008, **22**, 46–60.

52 F.V. Ferreira, D.R. Rocha and F. C. Silva, *Quim. Nova*, 2009, **32**, 623-638.

53 M. Sasaki, K. Takahashi, Y. Haneda, H. Satoh, A. Sasaki, A. Narumi, T. Satoh, T. Kakuchi and H. Kaga, *Carbohydrate Research*, 2008, **343**, 848–854.

54 F. S. Asghari and H. Yoshida, *Ind. Eng. Chem. Res*., 2006, **45**, 2163-2173.

55 A. Corma, S. Iborr and A. Velty, *Chem. Rev.,* 2007, **107**, 2411−2502.

56 P. Gallezot, *Chem. Soc. Ver.,* 2012, **41**, 1538-1558.

57 H. Kobayashi, Y. Yamakoshi, Y. Hosaka and M. Yabushita, *Catalysis Today,* 2014, **226**, 204-209.

58 P. L. Dhepe and A. Fukuoka, *Catal. Surv. Asia*. 2007, **11**, 186–191, 2007.

59 G. Zhao, M. Zheng, A. Wang and T. Zhang, *Chin. J. Catal*., 2010, **31**, 123-128.

60 M. K. Kim, P. S. Kim, J. H. Baik, I. S. Nam, B. K. Cho, S. H. Oh, *Applied Catalysis B: Environmental* , 2011, **105**, 171–181.

61 J.N. Díaz de León, M. Picquart, M. Villarroel, M. Vrinat, F.J. Gil Llambias, F. Murrieta and J.A. de los Reyes, *Journal of Molecular Catalysis A: Chemical*, 2010, **323**, 70–77.

62 A. Corma, *Chem. Rev*., 1995, **95**, 559.

TABLE CAPTIONS

Table 1

Ratio of Lewis/Brönsted acid sites (I_L/I_B) for the catalysts obtained from the pyridine-adsorbed infrared spectra.

FIGURE CAPTIONS

Figure 1

(a) Thermograms and (b) first-derivative curves (DrTGA) for the catalysts: MoO_3/TiO_2 - 30 , TiO_2 / SO_4^{2-}-25 and TiO_2 / SO_4^{2-} - 35.

Figure 2

Infrared absorption spectra for the catalysts: TiO_2/SO_4^{2-}-25, TiO_2/SO_4^{2-}-35 and TiO_2/MoO_3-30.

Figure 3

Raman spectra for TiO_2, TiO_2/SO_4^{2-}-25, TiO_2/SO_4^{2-}-35 and TiO_2/MoO_3-30.

Figure 4

Adsorbed – pyridine infrared spectra for catalysts at 190 °C.

Figure 5

(a) TPD-NH_3 analysis of TiO_2/MoO_3-30, TiO_2/SO_4^{2-}-25 and TiO_2/SO_4^{2}-35; (b) Acid strength of catalyst in reaction medium (calculated from peak area observed in the NH_3-TPD).

Figure 6

Cellulose conversion.

Figure 7

Yield of soluble products obtained in the cellulose conversion over the catalysts: TiO_2/ MoO_3- 30, TiO_2 / SO_4^{2-} - 25, TiO_2 / SO_4^{2}—35, TiO_2 and H_2SO_4, and without catalyst.

Table 1

Catalyst	I_L/I_B
TiO_2 / MoO_3 -30	0.60
TiO_2 / SO_4^{2-} -25	0.95
TiO_2 / SO_4^{2-} -35	1.02

Figure 1

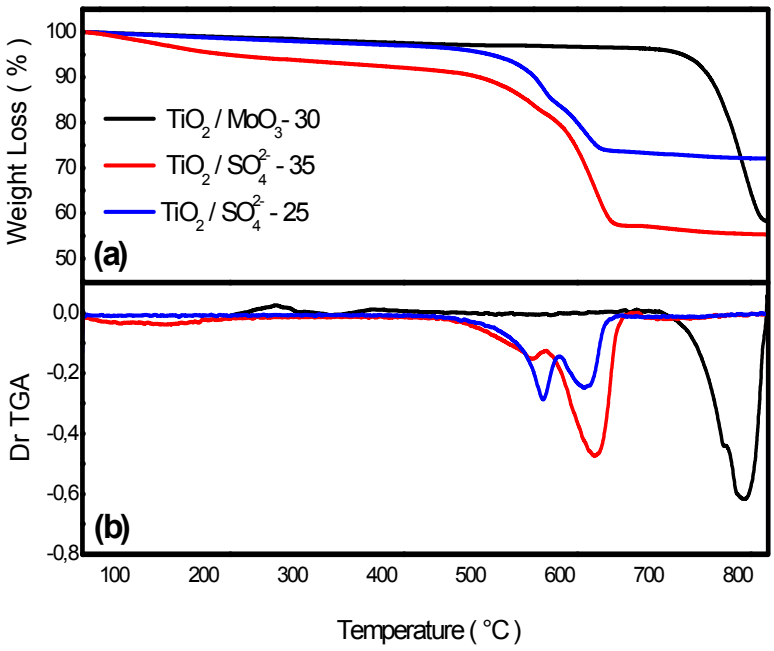

Figure 2

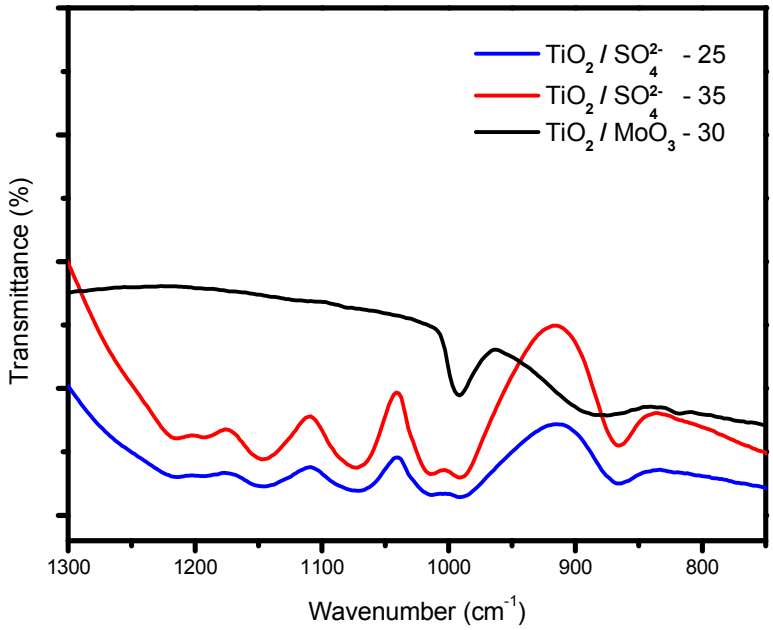

Figure 3

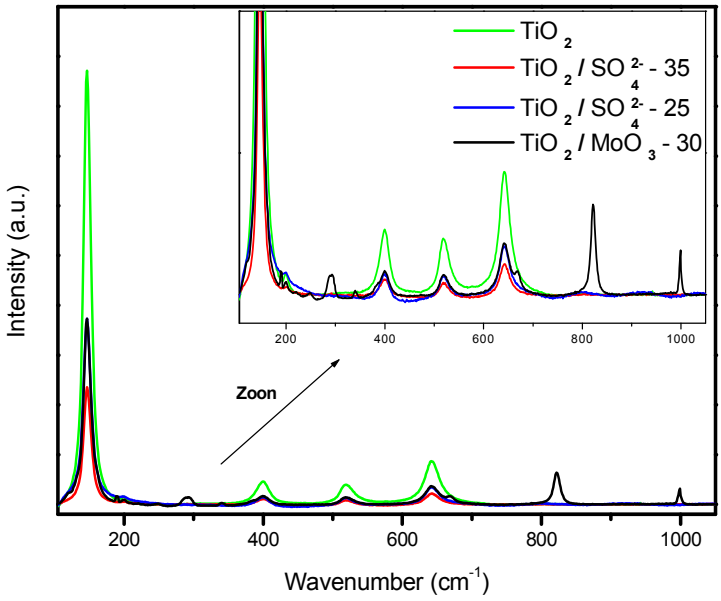

Figure 4

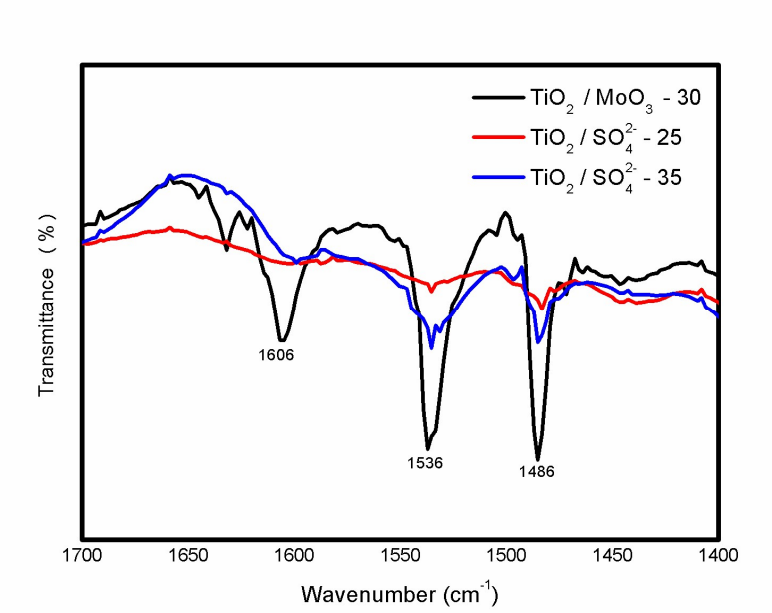

Figure 5

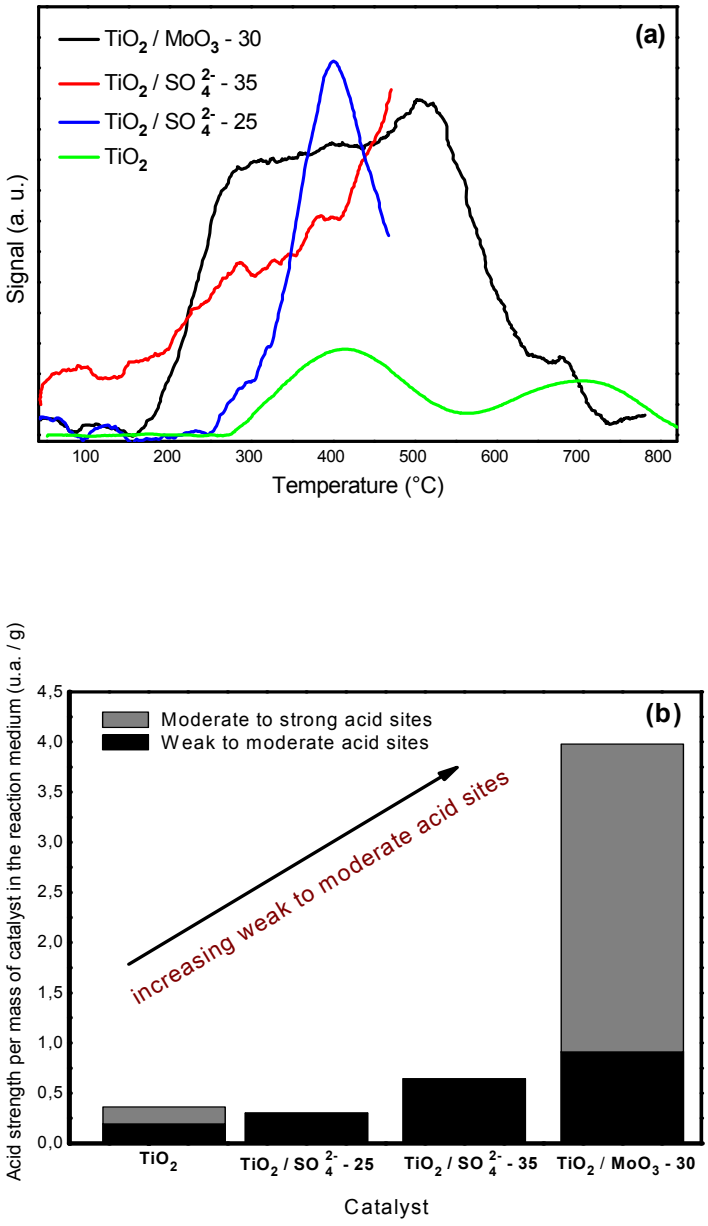

Figure 6

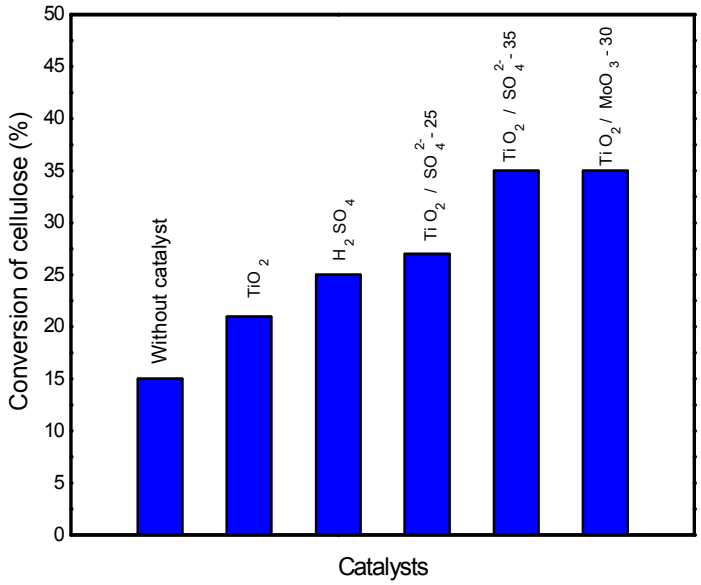

Figure 7